processes

MDPI

Article

Real-Time Optimization of Wastewater Treatment Plants via Constraint Adaptation

Ahteshamul Haq [1], Babji Srinivasan [2,*] and Dominique Bonvin [3]

[1] Department of Chemical Engineering, Indian Institute of Technology Gandhinagar, Gandhinagar 382355, India; ahteshamul.haq@iitgn.ac.in
[2] Department of Applied Mechanics, Indian Institute of Technology Madras, Chennai 600036, India
[3] Laboratoire d'Automatique, Ecole Polytechnique Fédérale de Lausanne, 1015 Lausanne, Switzerland; dominique.bonvin@epfl.ch
* Correspondence: babji.srinivasan@iitm.ac.in

Abstract: An important requirement of wastewater treatment plants (WWTPs) is compliance with the local regulations on effluent discharge, which are going to become more stringent in the future. The operation of WWTPs exhibits a trade-off between operational cost and effluent quality, which provides a scope for optimization. Process optimization is usually done by optimizing a model of the process. However, due to inevitable plant–model mismatch, the computed optimal solution is usually not optimal for the plant. This study represents the first attempt to handle plant–model mismatch via constraint adaptation (CA) for the real-time optimization of WWTPs. In this simulation study, the "plant" is a model adopted from the BSM1 benchmark, while a reduced-order "model" is used for making predictions and computing the optimal inputs. A first implementation uses steady-state measurements of the plant constraints to adjust the model in the optimization framework. A fast CA technique is also proposed, which adjusts the model using transient measurements. It is observed that, even in the presence of significant plant–model mismatch, the two proposed techniques are able to meet the active plant constraints. These techniques are found to reduce the pumping and aeration energy by 20%, as compared to that adopted in BSM1.

Keywords: WWTP; BSM1; real-time optimization; constraint adaptation; fast constraint adaptation

Citation: Haq, A.; Srinivasan, B.; Bonvin, D. Real-Time Optimization of Wastewater Treatment Plants via Constraint Adaptation. *Processes* **2022**, *10*, 990. https://doi.org/10.3390/pr10050990

Academic Editors: Francesca Raganati and Alessandra Procentese

Received: 7 April 2022
Accepted: 5 May 2022
Published: 17 May 2022

1. Introduction

Wastewater treatment plants (WWTPs) are large-scale facilities for restoring polluted wastewater to a desirable quality. Wastewater discharge standards are enforced to ensure a reduced environmental impact, the compliance of which are getting stricter with time. These stricter standards impose an extra burden on WWTPs, thus leading to a significant increase in their operational costs [1–3]. In the operation of a WWTP, most of the energy is consumed during the secondary treatment, where the majority of nutrients and organic matter is removed with the help of an activated sludge process. This energy, which consists of pumping energy for the recycle flows and aeration energy to provide oxygen to the aerobic processes, consumes 50–90% of the total electricity required for the plant [4–6]. The trade-off between cost (energy consumption) and treatment performance (effluent quality) can be addressed via optimization. In other words, optimal operation of WWTPs implies minimizing the operational cost, while complying with the wastewater discharge standards.

A major issue associated with the implementation of optimization techniques is casting a real-world problem into a mathematical model. Typically, a mathematical model cannot describe a real process (labeled here plant) accurately due to assumptions, approximations and simplifications associated with the modeling process. It follows that optimal solutions obtained by solving a model-based optimization problem are optimal for the model, but usually not for the plant due to inevitable plant–model mismatch. Furthermore, if these

model-based solutions are directly implemented on the plant, they may lead to violation of some key constraints. Unfortunately, this fact is too often overlooked by academic researchers. For example, there are several studies that propose to optimize the performance of WWTPs by solving a model-based optimization problem [6–11]. Additionally, some studies use model predictive controllers that rely on solving a model-based optimization problem [12–16]. Note, however, that the limitations of model-based approaches can be overcome by including plant measurements in the optimization framework to handle plant–model mismatch. These measurement-based optimization techniques are referred to as real-time optimization (RTO) in the literature [17,18].

Ideally, RTO techniques use plant measurements to drive the plant to optimality, while ensuring constraint satisfaction. Measurements can be used at three different levels, namely, the process model (to update the model parameters), the cost and constraints (to modify the cost and constraints of the optimization problem), and the constraints (to modify only the bias in the constraints of the optimization problem) as discussed next:

- Parametric uncertainties can be handled by updating the uncertain model parameters using a so-called "two-step" approach. This works well in the case of parametric plant-model mismatch, that is, when the plant-model mismatch can be corrected by parameter adaptation [19]. In the case of structural mismatch, parameter estimation will not be able to adapt the model correctly, and the two-step scheme may not work well [20].
- Structural uncertainty can be handled by modifying the cost and constraints of the optimization problem. The first investigation in this direction is the method labeled integrated system optimization and parameter estimation (ISOPE) [21]. However, the parameter estimation step makes its implementation difficult in the presence of measurement noise and insufficient excitation in the data. Hence, it may be beneficial to skip the parameter estimation step and modify only the cost and constraints in the optimization framework. The corrections added to the cost and constraints are referred to as modifier terms, and the resulting RTO scheme is named modifier adaptation (MA) [22]. The correction of bias and gradients in the predicted cost and constraints are performed via so-called zeroth- and first-order modifiers, respectively.
- When only zeroth-order modifiers are used to compensate for plant-model mismatch, the RTO method is known as constraint adaptation (CA) [23]. Note that gradient estimation is difficult in practice, especially with a large number of inputs. CA does not involve gradient estimation and is often preferred over MA. It ensures feasible operation of the plant by driving it iteratively to a point where all constraints are met. However, this way, optimal plant operation can only be ensured when the number of inputs (or decision variables) is equal to the number of active plant constraints [18].

This paper describes the application of CA towards the optimization of WWTPs. To the best of our knowledge, there is no work in the literature using CA for the real-time optimization of WWTPs. CA is an iterative scheme that ensures feasibility, but not necessarily optimality, upon convergence. However, in this study, since the optimal operation is characterized by two quality requirements (or constraints) being met, CA can lead to plant optimality by working with only two inputs.

Hence, CA is capable of optimizing the BSM1 plant operation at steady state using an adequate (but not necessarily accurate) model and appropriate either steady-state or transient measurements (There is a noticeable difference between model accuracy and model adequacy. In the context of MA and CA, good performance requires model adequacy, but not necessarily model accuracy. Model adequacy for CA simply says that the model is capable of predicting the correct set of active constraints at the plant optimum. See A.G. Marchetti, T. de Avila Ferreira, S. Costello and D. Bonvin, Modifier Adaptation as a Feedback Control Scheme, Ind. Eng. Chem. Res., 59(6), 2261–2274 (2020) for more details.). The reason for which plant optimality can be reached even with an inaccurate model is the fact that optimization is set up in a way that (i) the model is corrected using bias terms on the constraints so as to be able to predict the active plant constraints correctly,

and (ii) all degrees of freedom in the optimization problem are used to meet the active constraints [23]. Note that, this way, a higher priority is given to feasibility (meeting the active plant constraints) than to optimality, which corresponds to industrial practice.

The paper is organized as follows. Section 2 on Materials and Methods describes the various WWTP models, namely, the 147th-order BSM1 model, the 47th-order model that is used as "plant", and the 20th-order model that is used as "model". Then, the RTO methodologies CA and fast CA are briefly presented, first in general terms and then with respect to their application to WWTP. Section 3 on Results and Discussion presents the main results obtained with both CA and fast CA for the case of constant influents. Conclusions are provided in Section 4. In addition, there are three appendices supporting the model simplifications introduced to reduce the 147th-order BSM1 model to the 20th-order "model".

2. Materials and Methods

In silico approaches are often used to evaluate the performance of control and optimization schemes without expensive experimentation. For this, a simulated reality is typically selected as the "plant", as was done in [15,16]. These studies have considered the Benchmark Simulation Model No. 1 (BSM1) [24] as "plant" and a reduced-order model as "model". In our work, for simplicity, a 47th-order model adopted from the Benchmark Simulation Model No. 1 (BSM1) [24] is selected as "plant" and a reduced 20th-order model is used as "model" in CA schemes. The reason for this choice is twofold: (i) numerical optimization of the BSM1 model that includes the settler equations is a rather difficult task, and (ii) the actual performance of CA depends on the ability of a modified model to appropriately predicting the measured plant constraints; this is easily done by the use of bias terms that express the differences between the plant measurements and the values predicted by the model.

2.1. Wastewater Treatment Plant: Models and Controllers

Wastewater treatment is carried out in three main stages, namely, primary, secondary and tertiary treatments [25]. This study focuses on the secondary treatment that involves biological processes and secondary settling. The secondary treatment is also referred to as the activated sludge process (ASP) in the literature [26–30]. The standard benchmark model named BSM1 is widely used among the research community for simulation-based comparative studies.

2.1.1. Benchmark Simulation Model No. 1

The BSM1 model represents the activated sludge process in WWTPs, where the biological process is modeled using the Activated Sludge Model No.1 (ASM1) [31] and the settling process is modeled using the double-exponential settling velocity function [32]. BSM1, like any conventional secondary treatment in a WWTP, has a series of biological reactors followed by a settling tank. BSM1 includes 5 reactors, of which the first two are under anoxic conditions, and the remaining three are under aerobic conditions. The anoxic section, the aerobic section and the settler have capacities of 2000, 4000 and 6000 m^3, respectively. There are two recycle streams, namely, one from the last tank (labeled Q_a), and another one from the underflow of the settler (labeled Q_r). Furthermore, a WWTP typically involves two built-in control loops to regulate (i) the nitrate level in the second reactor, $S_{NOp,2}$, by manipulating Q_{ap}, and (ii) the oxygen level in the fifth reactor, $S_{Op,5}$, by manipulating the oxygen transfer coefficient $(K_La)_p$ in the aerobic section. This can be done using, for example, two proportional-integral (PI) controllers. The schematic representation of the BSM1 plant is shown in Figure 1.

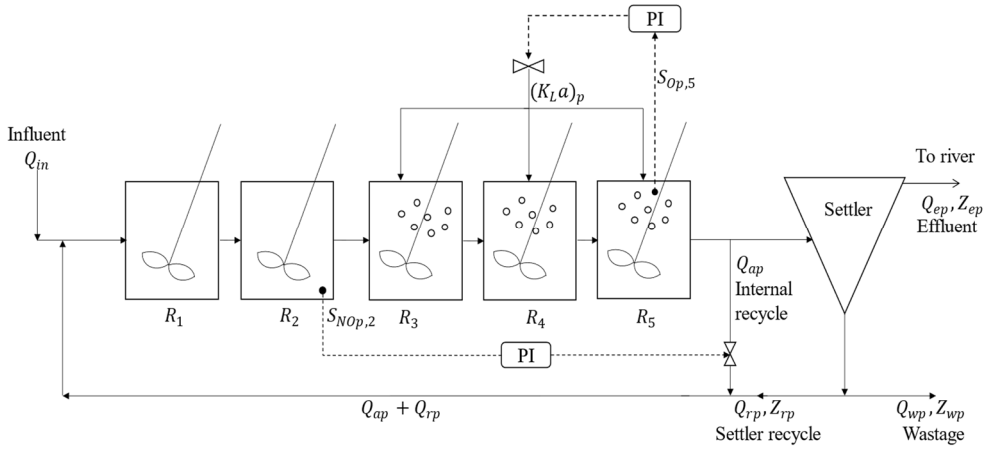

Figure 1. Schematic representation of the controlled BSM1 plant.

2.1.2. 47th-Order Plant Adopted from BSM1

In the BSM1 model, every biological reactor is described using 13 ordinary differential equations (ODEs). Hence, the series of five biological reactors contribute 65 ODEs to BSM1. The secondary settler is a ten-layer system, where each layer is represented by 8 ODEs. Hence, the secondary settler contributes 80 ODEs to BSM1. Furthermore, each controller adds one differential equation to the model if it possesses an integral term. Consequently, BSM1 has a total of 147 ODEs.

The settling process in BSM1 is assumed to be biologically inactive, which means there is no biological phenomena taking place in the settling tank, and the only process prevalent in the settler is the settling of solids. Consequently, the soluble matter concentrations are not affected by the settling process and are the same at both the inlet and the outlet of the settler. Moreover, the settler overflow has a negligible amount of particulate matter in the treated effluent, as can be seen in the simulated results presented in [24]. It follows that one can assume that the settler generates effluent with no particulate matter, which allows eliminating 80 ODEs from the BSM1 model. Hence, the assumption of a perfect settler in BSM1 reduces the number of ODEs from 147 to 67. The perfect settler equations are shown in Appendix A.

BSM1 can further be simplified by removing 20 additional ODEs from the model as each reactor contains two inert states and two so-called reaction invariants. Reaction invariants are state variables that are not directly affected by the reaction [33]. X_p and S_{Alk} are reaction invariants in ASM1 as they do not appear in the process rates shown in the ASM1 Peterson matrix presented in [31]. ASM1 also includes two inert states, S_I and X_I, which do not participate in the reactions and leave the system at their inlet concentrations. Removing the mass balance equations for these 4 states in each of the 5 biological reactor results in a 47th-order model. The representation of the reduced ASM1 model with 9 state variables in the form of Peterson matrix is shown in Appendix B. The 47th-order model presents two main advantages. Firstly, it is a good representation of BSM1 as its predictions are fairly close to those of the full model as shown in Table A1. Secondly, it can be easily optimized owing to the assumption of a perfect settler.

2.1.3. 20th-Order Model

The 47th-order "plant" model is still too large to be used for real-time computations. The model can be further simplified by combining the two anoxic reactors into a single reactor of volume 2000 m^3 and the three aerobic reactors into a single reactor of volume 4000 m^3. This way, a reduced model having only two reactors is obtained, with each reactor being represented by 9 ODEs. The reduced model includes 20 ODEs, 18 ODEs from the reactors and 2 ODEs from the PI controllers. This 20th-order model will be used as the "model" in the RTO scheme. The schematic representation of this controlled model is shown in Figure 2.

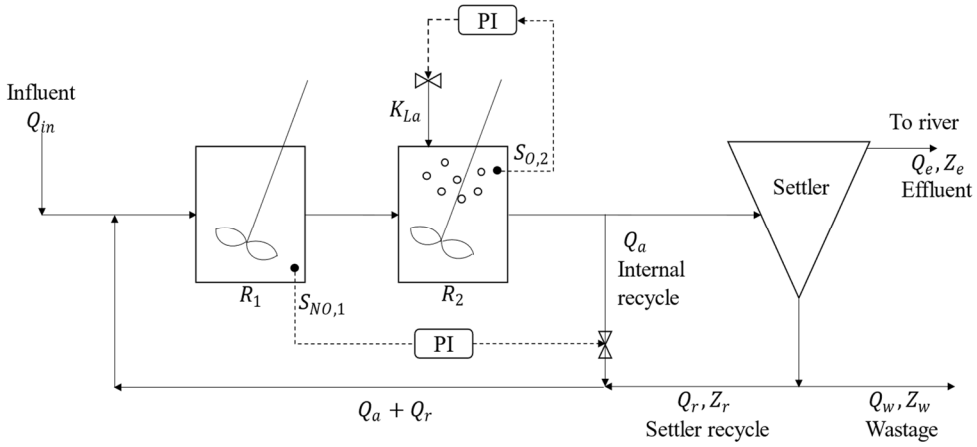

Figure 2. Schematic representation of the controlled 20th-order model.

2.1.4. Design of Controllers

The general equation for a PI controller is given as [34]:

$$u(t) = K_c\left(e(t) + \frac{1}{\tau_I}\int_0^t e(t)dt\right) \tag{1}$$

where u is the manipulated variable, e is the difference between the setpoint (SP) and the process variable (PV), K_c is the controller gain and τ_I is the integral time constant.

Differentiating Equation (1) with respect to t gives the following ODE:

$$\dot{u}(t) = K_c\left(\dot{e}(t) + \frac{1}{\tau_I}e(t)\right) \tag{2}$$

Based on this equation, the controller equations for the plant and the model are provided in Appendix C. Controller tuning can be done using, for example, the Ziegler–Nichols step response method [34].

2.2. RTO via Constraint Adaptation

2.2.1. Formulation of the Optimization Problem

Let the steady-state plant optimization problem be expressed mathematically as [35]:

$$\begin{aligned} \boldsymbol{u}_p^* arg\ \min_{\boldsymbol{u}} & \Phi_p(\boldsymbol{u})\phi_p\left(\boldsymbol{u}, \boldsymbol{y}_p(\boldsymbol{u})\right) \\ s.t.\ \ & \boldsymbol{G}_p(\boldsymbol{u})\boldsymbol{g}_p\left(\boldsymbol{u}, \boldsymbol{y}_p(\boldsymbol{u})\right) \leq \boldsymbol{0} \\ & \boldsymbol{u}^L \leq \boldsymbol{u} \leq \boldsymbol{u}^U \end{aligned} \tag{3}$$

where $\boldsymbol{u}$ is the input vector of dimension n_u, $\boldsymbol{y}_p$ is the measured plant output vector of dimension n_y, ϕ_p is the plant cost function, $\boldsymbol{g}_p$ is the vector of plant constraints of dimension n_G, and subscript $(\cdot)_p$ indicates a quantity related to the plant. Furthermore, Φ_p and $\boldsymbol{G}_p$ are the plant cost function and vector of plant constraints expressed in terms of $\boldsymbol{u}$, respectively.

It is clear in the above definitions that the plant cost and constraints are known function of $\boldsymbol{u}$ and $\boldsymbol{y}_p$. However, in practice, the plant steady-state input–output mapping $\boldsymbol{y}_p(\boldsymbol{u})$ is typically unknown, and it is estimated using an approximate steady-state model:

$$\boldsymbol{f}(\boldsymbol{x}, \boldsymbol{u}, \boldsymbol{\theta}) = \boldsymbol{0} \tag{4}$$

$$\boldsymbol{y} = \boldsymbol{h}(\boldsymbol{x}, \boldsymbol{u}, \boldsymbol{\theta}) \tag{5}$$

where $\boldsymbol{x}$ is the state vector of dimension n_x, $\boldsymbol{y}$ is the model predicted outputs vector of dimension n_y, and $\boldsymbol{\theta}$ is the model parameters vector of dimension n_θ.

Solution to $\boldsymbol{f}(\boldsymbol{x}, \boldsymbol{u}, \boldsymbol{\theta}) = \boldsymbol{0}$ can be expressed as $\boldsymbol{x} = \boldsymbol{\xi}(\boldsymbol{u}, \boldsymbol{\theta})$ with $\boldsymbol{\xi}$ the steady-state map between $\boldsymbol{u}$ and $\boldsymbol{x}$. Hence, the input–output map predicted by the model can be represented as:

$$\boldsymbol{y}(\boldsymbol{u}, \boldsymbol{\theta}) = \boldsymbol{h}(\boldsymbol{\xi}(\boldsymbol{u}, \boldsymbol{\theta}), \boldsymbol{u}, \boldsymbol{\theta}) = \boldsymbol{H}(\boldsymbol{u}, \boldsymbol{\theta}) \tag{6}$$

This way, a model-based optimization problem can be formulated as follows:

$$\begin{gathered} \boldsymbol{u}^* \arg\min_{u} \phi(\boldsymbol{u}, \boldsymbol{\theta}) \phi(\boldsymbol{u}, \boldsymbol{y}(\boldsymbol{u}, \boldsymbol{\theta})) \\ s.\, t. \boldsymbol{G}(\boldsymbol{u}, \boldsymbol{\theta}) \boldsymbol{g}(\boldsymbol{u}, \boldsymbol{y}(\boldsymbol{u}, \boldsymbol{\theta})) \leq \boldsymbol{0} \\ \boldsymbol{u}^L \leq \boldsymbol{u} \leq \boldsymbol{u}^U \end{gathered} \tag{7}$$

where ϕ is the model cost function, $\boldsymbol{g}$ is the vector of model constraints of dimension n_G, Φ is the plant cost function expressed in terms of $\boldsymbol{u}$, and $\boldsymbol{G}$ is the vector of plant constraints expressed in terms of $\boldsymbol{u}$.

The model-based optimization problem Equation (7) can be solved numerically. However, the model optimum $\boldsymbol{u}^*$ does not coincide with plant optimum $\boldsymbol{u}_p^*$ due to plant–model mismatch. Hence, plant measurements are incorporated into the optimization framework to tackle this plant–model mismatch. In CA, these measurements are used to construct zeroth-order modifiers. Zeroth-order modifiers are used for bias correction in the predicted constraints. They represent the difference between the measured plant constraints and the constraints predicted by the model for given inputs. There is no need to add zeroth-order modifier to the cost function since adding a constant value to the cost function does not change the location of the optimal solution. Hence, it is used only with the constraints and computed as follows:

$$\boldsymbol{\epsilon}_k^G = \boldsymbol{G}_p(\boldsymbol{u}_k) - \boldsymbol{G}(\boldsymbol{u}_k, \boldsymbol{\theta}) \tag{8}$$

where $\boldsymbol{\epsilon}_k^G$ is a vector of dimension n_G, and k is the iteration number.

2.2.2. CA Using Steady-State Measurements

Using the aforementioned zeroth-order modifiers, a modified optimization problem is solved iteratively as per Figure 3. At kth RTO iteration, $\boldsymbol{u}_k$ is obtained from the numerical solution to the following modified optimization problem:

$$\begin{gathered} \boldsymbol{u}_{k+1} := \operatorname{argmin}_{u} \Phi(\boldsymbol{u}) \\ s.t.\ \boldsymbol{G}_m(\boldsymbol{u}) := \boldsymbol{G}(\boldsymbol{u}) + \boldsymbol{\epsilon}_{f,k}^G \leq \boldsymbol{0} \end{gathered} \tag{9}$$

where $\boldsymbol{\epsilon}_{f,k}^G$ are filtered modifiers as discussed next, and subscript $(\cdot)_m$ indicates a quantity that has been modified. Indeed, using modifiers Equation (8) often results in overcorrection, thereby causing the CA scheme to oscillate. This can be avoided by applying a first-order filter on the modifiers as follows:

$$\boldsymbol{\epsilon}_{f,k}^G = (\boldsymbol{I} - \boldsymbol{K}) \boldsymbol{\epsilon}_{f,k-1}^G + \boldsymbol{K} \boldsymbol{\epsilon}_k^G \tag{10}$$

$\boldsymbol{I}$ is the identity matrix, while $\boldsymbol{K}$ is a filter matrix whose eigenvalues are between 0 (full filtering) and 1 (no filtering). The matrix $\boldsymbol{K}$ is often chosen as a diagonal matrix, with n_G identical eigenvalues, that is, $\boldsymbol{K} = K\boldsymbol{I}$. The more noise, the lower the K value. Values between 0.5 and 0.8 are often used. The effect of more filtering is to reduce the convergence speed, but it does not affect the converged values. The CA algorithm is given next:

1. Initialize the filtered modifiers $\boldsymbol{\epsilon}_{f,0}^G = \boldsymbol{0}$. Choose the filter matrix $\boldsymbol{K}$ and the convergence threshold δ. Set $k0$.
2. Solve the modified optimization problem Equation (9) to get the inputs $\boldsymbol{u}_{k+1}$.
3. If $\|\boldsymbol{u}_{k+1} - \boldsymbol{u}_k\| \leq \delta$, set $kk + 1$; otherwise stop.
4. Apply the inputs to the plant, wait for steady state and take the measurements $\boldsymbol{G}_p(\boldsymbol{u}_k)$.
5. Evaluate the modifiers Equation (8), apply the filter Equation (10) and return to Step 2.

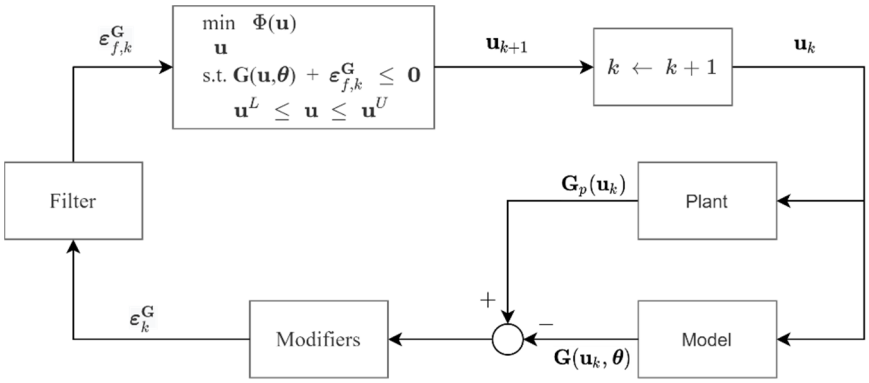

Figure 3. Block diagram of the CA algorithm.

If the above RTO scheme converges, it will satisfy the plant constraints. For instance, if the RTO scheme converges for $k \to \infty$, then the modified quantities for $k \to \infty$ correspond to the plant quantities, and $\boldsymbol{G}_m$ approaches $\boldsymbol{G}_p$ as shown below:

$$\begin{aligned} \boldsymbol{G}_m(\boldsymbol{u}, \boldsymbol{y}(\boldsymbol{u}_\infty, \boldsymbol{\theta})) &:= \boldsymbol{G}(\boldsymbol{u}_\infty, \boldsymbol{y}(\boldsymbol{u}_\infty, \boldsymbol{\theta})) + \boldsymbol{\epsilon}^G_\infty \\ \boldsymbol{G}_m(\boldsymbol{u}, \boldsymbol{y}(\boldsymbol{u}_\infty, \boldsymbol{\theta})) &:= \boldsymbol{G}(\boldsymbol{u}_\infty, \boldsymbol{y}(\boldsymbol{u}_\infty, \boldsymbol{\theta})) + \boldsymbol{G}_p\Big(\boldsymbol{u}_\infty, \boldsymbol{y}_p(\boldsymbol{u}_\infty)\Big) - \boldsymbol{G}(\boldsymbol{u}_\infty, \boldsymbol{y}(\boldsymbol{u}_\infty, \boldsymbol{\theta})) \\ \boldsymbol{G}_m(\boldsymbol{u}, \boldsymbol{y}(\boldsymbol{u}_\infty, \boldsymbol{\theta})) &:= \boldsymbol{G}_p\Big(\boldsymbol{u}_\infty, \boldsymbol{y}_p(\boldsymbol{u}_\infty)\Big) \end{aligned}$$

2.2.3. Fast CA Using Transient Measurements

CA solves a modified optimization problem that uses steady-state plant measurements. When the plant requires much time to reach steady-state, this results in slow convergence to plant optimality. This issue can be mitigated by *estimating* the plant steady state using transient measurements and a dynamic model as shown in Figure 4 [36,37]. For this, at time t_k corresponding to the kth RTO iteration during transient, the plant measurements y_p^{dyn} are taken and complemented by the model prediction of the remaining part of the transient to steady state. This prediction Δ is obtained via a dynamic model of the plant. Hence, an estimate of the plant steady-state y_p^{ss} is obtained as:

$$\hat{y}_p^{SS} = y_p^{dyn} + \Delta = y_p^{dyn} + \left(y^{SS} - y^{dyn}\right) \tag{11}$$

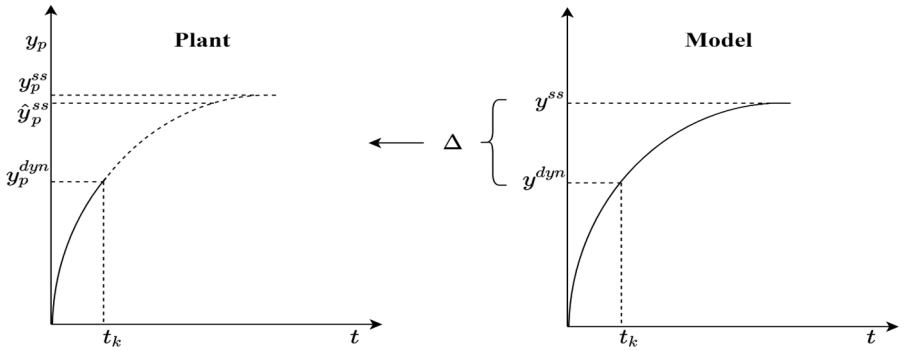

Figure 4. Estimation of plant steady state using measurements and a dynamic model.

The estimated plant steady state is used in the CA scheme, which can then converge in a single settling time (i.e., the time it takes for the plant to reach steady state). CA using transient measurements is referred to as fast CA in the literature [38].

Both CA and fast CA ensure feasible operation of the plant by driving it iteratively to a point where all the constraints are met. In some cases, it also provides plant optimality, in particular when the number of active constraints is equal to the number of inputs [23].

Note that both CA and fast CA need to work iteratively because they compute an optimum locally (and not globally) at each iteration.

2.3. RTO Applied to WWTP

This section describes the application of RTO to a WWTP as per the scheme shown in Figure 3. The optimization problem is solved by incorporating the model described in Section 2.1.3. as equality constraints. This model is also used to provide the model predictions needed to compute the modifiers. The plant measurements required in the RTO scheme are generated by simulating the plant described in Section 2.1.2. In addition, a plant optimization problem is solved to determine the plant optimum, which is required to verify that the RTO scheme reaches plant optimality. As highlighted earlier, the mechanical pumping and the aeration process are the two most energy-intensive processes in WWTPs. Hence, the objective of optimization is to minimize the sum of pumping energy (PE) and aeration energy (AE) of the WWTP as presented below.

PE, which represents the energy used for pumping the internal recycle stream Q_a, is calculated as follows:

$$\text{PE} = f_{PE} \cdot Q_a \qquad \left[\text{kWh} \cdot \text{d}^{-1}\right] \tag{12}$$

where f_{PE} is the PE factor and has the value of 0.004 $\text{kWh} \cdot \text{m}^{-3}$ as given in [24].

AE is expressed in terms of the oxygen transfer coefficient K_La and represents the energy needed to transfer oxygen into the reactor. K_La is directly related to energy-consuming factors such as airflow and mixing velocity [39]. It is assumed that 1800 gO_2 can be transferred per kWh of energy at 15 °C and zero dissolved oxygen concentration [24]. This assumption leads to the following oxygen transfer rate (OTR) expression:

$$\text{OTR} = V_{aerobic} \cdot K_La \cdot S_{O,sat} \qquad \left[\text{gO}_2 \cdot \text{d}^{-1}\right] \tag{13}$$

where $V_{aerobic}$ is the volume of the reactor under aerobic conditions expressed in m^{-3}, and $S_{O,sat}$ is the oxygen saturation concentration with the value of 8 $\text{gO}_2 \cdot \text{m}^{-3}$ at 15 °C. Hence, AE can be calculated as follows:

$$\text{AE} = f_{AE} \cdot \text{OTR} \qquad \left[\text{kWh} \cdot \text{d}^{-1}\right] \tag{14}$$

where f_{AE} is the AE factor and has the value of $\frac{1}{1800}$ $\text{kWh} \cdot (\text{g O}_2)^{-1}$ as provided in [24].

Finally, the overall cost index (OCI) is expressed as the sum of PE and AE:

$$\text{OCI} = 0.004\ Q_a + \frac{S_{O,sat}}{1800} \cdot V_{aerobic} \cdot K_Latext \qquad \left[\text{kWh} \cdot \text{d}^{-1}\right] \tag{15}$$

Substituting $S_{O,sat} = 8$ and $V_{aerobic} = 4000$ in the above expression gives:

$$\text{OCI} = 0.004\ Q_a + 17.8 K_La \qquad \left[\text{kWh} \cdot \text{d}^{-1}\right] \tag{16}$$

The constraints for the optimization problems include bounds on the manipulated variables K_La and Q_a and on the setpoints of the controlled variables spS_{NO} and spS_O. Additionally, a constraint is also placed on the ammonia concentration in the effluent. Constraint adaptation guarantees feasible operation upon convergence; therefore, the bounds are not going to be violated. Hence, the effluent quality (EQ) is automatically enforced by the upper bounds on the concentrations. The various optimization problems can be formulated as discussed next.

2.3.1. Plant Optimization Problem

The plant optimization problem is solved to have some prior knowledge of plant optimality in this simulation study. The plant optimum will be used to validate the optimum obtained using RTO schemes. The plant optimization problem reads:

$$\begin{gathered} \min_{spS_{NOp,2}, spS_{Op,5}} \quad 0.004Q_{ap} + 17.8(K_La)_p \\ 45\ SS\ plant\ equations \\ 2\ SS\ controller\ equations \\ 180 \leq Q_{ap} \leq 92,000 \\ 1.5 \leq (K_La)_p \leq 360 \\ 0.5 \leq spS_{NOp,2} \leq 5 \\ 0.5 \leq spS_{Op,5} \leq 5 \\ S_{NHp,5} \leq 4 \end{gathered} \tag{17}$$

This optimization problem is formulated with the setpoints $spS_{NOp,2}$ and $spS_{Op,5}$ as decision variables and includes bounds on the inputs Q_{ap} and $(K_La)_p$. These bounds are adopted from [24]. In Equation (17), SS stands for steady state and the optimization problem includes 45 steady-state plant equations along with 2 controller equations as constraints.

2.3.2. Model Optimization Problem

The model optimization problem includes 18 steady-state model equations along with 2 steady-state controller equations as constraints as represented below:

$$\begin{gathered} \min_{spS_{NO,1},\ spS_{O,2}} \quad 0.004Q_a + 17.8K_La \\ 18\ SS\ model\ equations \\ 2\ SS\ controller\ equations \\ 180 \leq Q_a \leq 92,000 \\ 1.5 \leq K_La \leq 360 \\ 0.5 \leq spS_{NO,1} \leq 5 \\ 0.5 \leq spS_{O,2} \leq 5 \\ S_{NH,2} \leq 4 \end{gathered} \tag{18}$$

The bounds on inputs and setpoints of the model optimization problem are taken similar to that of the plant as described in the Section 2.3.1. In the presence of plant-model mismatch, the optimal solution to the above model-based problem does not typically lead to plant optimality. Hence, the model-based problem will be modified and used in the CA and fast CA schemes to drive the plant towards optimality.

2.3.3. Modified Optimization Problem

The following modified optimization problem is solved at each RTO iteration k to compute the optimal setpoints for the next iteration:

$$\begin{gathered} \min_{spS_{NO,1},\ spS_{O,2}} \quad 0.004Q_a + 17.8K_La \\ 18\ SS\ model\ equations \\ 2\ SS\ controller\ equations \\ 180 \leq Q_a \leq 92,000 \\ 1.5 \leq K_La \leq 360 \\ 0.5 \leq spS_{NO,1} \leq 5 \\ 0.5 \leq spS_{O,2} \leq 5 \\ S_{NH,2} + \epsilon_k \leq 4 \end{gathered} \tag{19}$$

When some of the constrained quantities are either perfectly known or known functions of the inputs, they possess no uncertainty and thus they do not require modification [40]. The bounds on the inputs Q_a and K_La represent saturations of the control actions. These saturation limits are perfectly known. In addition, the bounds on the setpoints are also perfectly known. Consequently, the bounds on inputs and setpoints need not be modified in the RTO scheme. Hence, $S_{NH,2}$ is the only quantity that needs to be modified via zeroth-order modifier as described next.

Zeroth-order modifier for CA

The inequality constraint G in a minimization problem formulation is typically provided by specifying an upper bound at zero, that is, $G \leq 0$. Consequently, the upper bounds on the ammonia concentrations can be expressed as follows:

$$G_p := S_{NHp,5} - 4 \leq 0 \tag{20}$$

$$G := S_{NH,2} - 4 \leq 0 \tag{21}$$

The zeroth-order modifier is then expressed using steady-state measurements as:

$$\epsilon_k^G = G_p - G = S_{NHp,5} - S_{NH,2} \tag{22}$$

Zeroth-order modifier for fast CA

Fast CA uses transient measurements denoted $(\cdot)_{dyn}$, and the steady state of the plant is estimated using a dynamic model. For example, the steady-state value of G_p can be estimated using Equation (11) as follows:

$$\hat{G}_p = G_p^{dyn} + \left(G - G^{dyn}\right) \tag{23}$$

The zeroth-order modifier can then be evaluated as:

$$\hat{\epsilon}_k = \hat{G}_p - G \ = G_p^{dyn} - G^{dyn} = S_{NHp,5}^{dyn} - S_{NH,2}^{dyn} \tag{24}$$

3. Results and Discussion

This study assumes that a constant influent is treated by the WWTP. This influent is adopted from [24], and its parameters are given in Table 1.

Table 1. Constant influent data.

Variables	S_S	X_S	X_{BH}	S_{NH}	S_{ND}	X_{ND}	Q_{in}
Values	69.5	202.32	28.17	31.56	6.95	10.59	18,446
Units	g COD·m^{-3}	g COD·m^{-3}	g COD·m^{-3}	g N·m^{-3}	g N·m^{-3}	g N·m^{-3}	m^3/d

$S_O = 0$ g COD·m^{-3}, $X_{BA} = 0$ g COD·m^{-3}, $S_{NO} = 0$ g N·m^{-3}.

The control parameters for both the plant and the model are obtained using the Control Systems Toolbox in MATLAB©. First, single-input, single-output models are obtained in the form of transfer functions using step responses. This is followed by the design of two PI controllers. The control parameters for the plant and the model are given in Table 2.

Table 2. Control parameters for the model and plant.

Control Parameters	K_{C1}	τ_{I1}	K_{C2}	τ_{I2}
Plant controllers	294	0.0069	4.7	0.066
Model controllers	122.8	0.0035	2.6	0.024

When the BSM1 control strategy presented in [24] is applied to the 47th-order plant for regulating the concentration of $S_{NOp,2}$ at 1 g N/m^3 by manipulating Q_a and that of $S_{Op,5}$ at

2 g COD/m^3 by manipulating K_La in the fifth reactor, the plant OCI is 3674 kWh·d^{-1}. Note that K_La for the third and fourth reactors are fixed at 240 d^{-1}, similar to those in BSM1.

This work uses the CasADi framework [41] to solve the numerical optimization problems. The variables of interest corresponding to the plant optimum are reported in Table 3. These results will be used to validate the converged CA and fast CA solutions.

Table 3. Plant steady-state optimization results.

Variables	$spS_{NOp,2}$	$spS_{Op,5}$	$S_{NHp,5}$	Q_{ap}	$(K_La)_p$	OCI_p
Plant SS values	0.5	0.81	4	34,460.9	153.81	2872.2
Units	g N·m^{-3}	g COD·m^{-3}	g N·m^{-3}	m^3/d	1/d	kWh/d

The variables of interest corresponding to the model optimum are reported in Table 4. These setpoints are implemented on the plant to show the consequence of direct application of the model optimum to the plant.

Table 4. Model steady-state optimization results.

Variables	$spS_{NO,1}$	$spS_{O,2}$	$S_{NH,2}$	Q_a	K_La	OCI
Model SS values	0.5	0.76	4	20,321.5	159.32	2913.6
Units	g N·m^{-3}	g COD·m^{-3}	g N·m^{-3}	m^3/d	1/d	kWh/d

As highlighted earlier, operating the plant using the model-based optimal setpoints results in suboptimal operation. In the worst case, it may even lead to infeasible plant operation due to plant–model mismatch. Such an instance is shown in Table 5. It can be observed that $S_{NHp,5} > 4$, thereby representing infeasible plant operation at the model optimum.

Table 5. Plant steady-state values at model optimum.

Variables	$spS_{NOp,2}$	$spS_{Op,5}$	$S_{NHp,5}$	Q_{ap}	$(K_La)_p$	OCI_p
Plant SS values	0.5	0.76	4.65	38,636.3	151.53	2848.4
Units	g N·m^{-3}	g COD·m^{-3}	g N·m^{-3}	m^3/d	1/d	kWh/d

The characterization of the model optimal solution (Table 4) indicates that two constraints are active at the optimum, namely, $spS^*_{NO,1} = 0.5$ and $S^*_{NH,2} = 4$. Since the optimization problem has two decision variables, optimality is completely determined by these two active constraints. Hence, updating Q_a and K_La to meet these two optimality-determining quantities will drive the plant towards optimality.

CA scheme. Plant optimality can be verified by the CA results in Figures 5 and 6. The red-dotted lines in Figure 5 represent the plant optimal values obtained by solving Equation (17), whereas in Figure 6 they represent the bounds on the nitrate, oxygen and ammonia concentrations. RTO is started from the steady-state values achieved by implementing the BSM1 control strategy to the plant. It can be observed that the CA scheme takes two iterations (around 120 days) to drive the plant close to optimality, where blue RTO lines overlap the red-dotted plant optimal lines. We notice here an important dichotomy, namely, two iterations are indicative of quick convergence, whereas 120 days is an unacceptable long time! This is due to the long time (60 days) taken by the plant to reach steady state following a system perturbation. This long settling time is intrinsic to WWTPs and cannot be changed with RTO schemes that rely on steady-state measurements. However, the practical message that can be taken from Figures 5 and 6 is the following: CA updates the setpoints $spS_{NO,1}$ and $spS_{O,2}$ for the model (or $spS_{NOp,2}$ and $spS_{Op,5}$ for the plant and thus also Q_{ap} and $(K_La)_p$ via the two PI controllers) in a direction that improves the OCI. Another message is that it would be quite useful in WWTP to be able to use transient

measurements in order to avoid having to wait so long for steady state. This is precisely what fast CA does, as shown next.

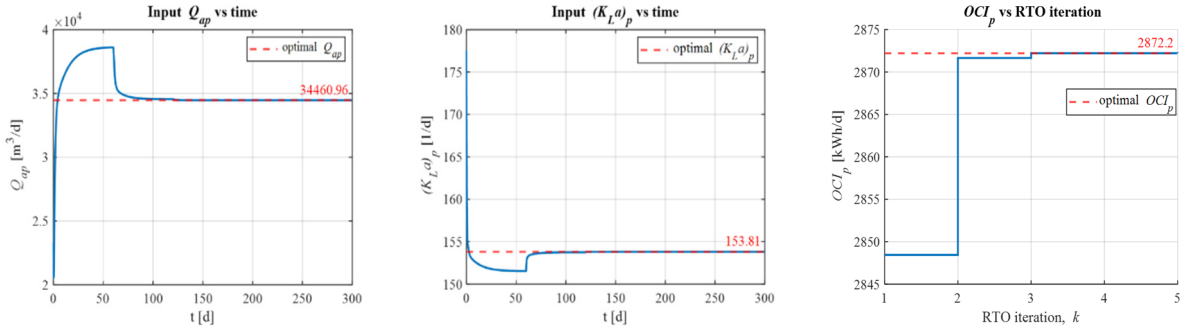

Figure 5. CA results–Plant inputs and overall cost index.

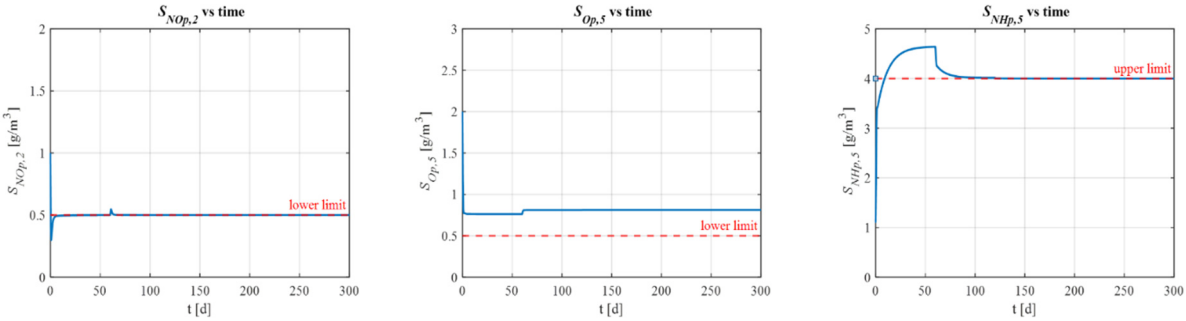

Figure 6. CA results–Plant variables.

Fast CA scheme. Plant optimality can be achieved in a single settling time using the fast CA approach as shown in Figures 7 and 8. Blue-solid and red-dotted lines in these figures represent the same as they do in Figures 5 and 6. The time between transient measurements, τ_{RTO}, is chosen to be 1 day. It can be noticed that the plant reaches optimality within about 50 days, where the blue RTO lines overlap the red-dotted plant optimal lines. The value of the filter K for the CA and the fast CA is chosen to be 0.6 and 0.5, respectively.

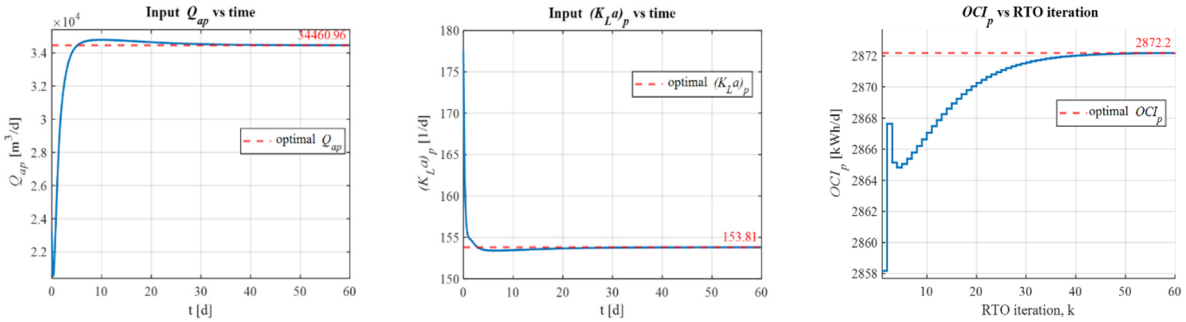

Figure 7. Fast CA results–Plant inputs and overall cost index.

There are three constrained quantities in the optimization problem, namely, $spS_{NO,1}$, $spS_{O,2}$ and $S_{NH,2}$. The beauty of the adopted strategy is illustrated by the fact that, if two of the constraints are active at the optimum, the PI controllers can directly drive the plant to optimality in a single RTO iteration. Note, however, that feasibility is not ensured prior to convergence. This is clearly seen with CA in Figure 6, with the ammonia concentration exceeding its upper limit in the time period $10 < t < 80$ d. In contrast, fast CA, which relies on most frequent measurements, is less aggressive and thus does not exhibit overshoot and constraint violation at all (see Figure 8).

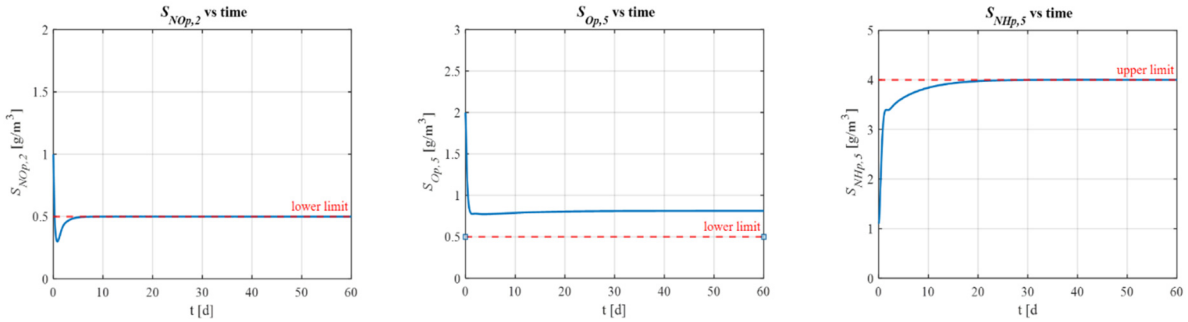

Figure 8. Fast CA results—Plant variables.

4. Conclusions

The work has considered the real-time operation of WWTPs at minimal energy cost, while still satisfying the effluent discharge norms. It has been proposed to incorporate plant measurements in a model-based optimization framework in order to drive the plant to plant optimality. The two methods investigated here are CA and fast CA that both use measurements of the constrained quantities for bias correction in the optimization framework.

The procedure is iterative because the model correction at each iteration is only locally (and not globally) correct. By design, CA ensures feasibility upon convergence. In addition, it can drive the plant to optimality when the number of active constraints is equal to that of decision variables. This is precisely the case in this study of WWTPs, and it is observed that the pumping and aeration energy can be reduced by about 20% as compared to the BSM1 control strategy, while still satisfying the requirement on ammonia concentration in the effluent.

In this work, the plant is considered to treat an influent of constant flow and composition. Most of the WWTPs have a buffer system or equalization tank to feed a constant flow and composition influent to the WWTP. Nevertheless, the influent coming to the WWTP has time-varying flowrate and composition. For time-varying influent, the proposed methodology can, in principle, still be implemented to reach plant optimality. However, this would call for the online solution to a dynamic (rather than static) optimization problem, a much more challenging task, which could be the subject of further research.

Another topic of considerable interest is the possibility of using machine-learning techniques for the modeling, estimation and optimization of WWTPs. However, one has to keep in mind that these techniques need to rely on "representative measurements" in order to perform well. In the case of WWTPs, representative measurements probably need to include the various concentrations, which unfortunately are rarely available as a whole. Hence, whether machine-learning techniques are suited to tackle real WWTPs is still an open question. A few preliminary research results are available, see for example [42–44].

Author Contributions: Conceptualization, A.H., B.S. and D.B.; methodology, A.H.; software, A.H.; validation, A.H., B.S. and D.B.; formal analysis, A.H. and D.B.; investigation, A.H.; resources, B.S. and D.B.; data curation, A.H. and B.S.; writing—original draft preparation, A.H.; writing—review and editing, A.H., B.S. and D.B.; visualization, A.H.; supervision, B.S. and D.B.; project administration, B.S.; funding acquisition, B.S. All authors have read and agreed to the published version of the manuscript.

Funding: This research received no external funding.

Institutional Review Board Statement: Not applicable.

Informed Consent Statement: Not applicable.

Data Availability Statement: Not applicable.

Conflicts of Interest: The authors declare no conflict of interest.

Appendix A

Perfect Settler

As shown in the figure below, a portion of the stream, namely Q_a, is removed from the flow Q_5 leaving the fifth reactor and recycled to the first reactor. The remaining part of Q_5 is sent to the settler as the feed Q_f. The concentration of Q_f is the same as that of Q_5.

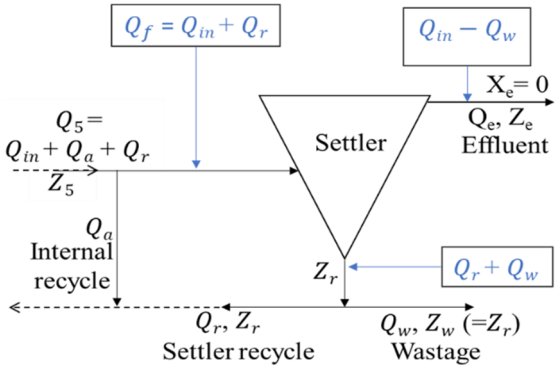

Figure A1. Schematic representation of a perfect settler. Symbols: Q_f: Settler feed flowrate, Q_{in}: Influent flowrate, Q_a: Internal recycle flowrate, Q_5: Flow from reactor 5, Z_5: Concentration in Q_5, Q_r: External recycle flowrate, Z_r: Concentration in Q_r, Q_e: Effluent flowrate, Z_e: Concentration in Q_e, Q_w: Wastage sludge flowrate, and Z_w: Concentration in Q_w.

The concentration of the settler underflow, Z_r, can be expressed in terms of Q_r and Q_w as shown next:

$$(Q_{in} + Q_r) \cdot Z_5 = (Q_{in} - Q_w) \cdot Z_e + (Q_r + Q_w) \cdot Z_r \tag{A1}$$

- For the soluble matter (S), $S_e = S_5$

$$S_r = \frac{(Q_{in} + Q_r)S_5 - (Q_{in} - Q_w)S_5}{(Q_r + Q_w)} = S_5 \tag{A2}$$

- For the particulate matter (X), $X_e = 0$

$$X_r = \frac{(Q_{in} + Q_r)X_5 \cdot (Q_{in} - Q_w) \times 0}{(Q_r + Q_w)} = \frac{(Q_{in} + Q_r)}{(Q_r + Q_w)} \cdot X_5 \tag{A3}$$

$$factor = \frac{(Q_{in} + Q_r)}{(Q_r + Q_w)} \tag{A4}$$

Hence, the external recycle has the following characteristics: flowrate, Q_r; soluble matter concentration, $S_r = S_5$ and particulate matter concentration, $X_r = factor \times X_5$.

Table A1. Steady-state values of variables of interest of the 147th-order and 47th-order models at three different set of inputs.

Variables	Units	147th-Order Model	47th-Order Model	147th-Order Model	47th-Order Model	147th-Order Model	47th-Order Model
Q_{ap}	m^3/d	55,338	55,338	36,892	36,892	18,446	18,446
$(K_La)_p$	1/d	240	240	200	200	160	160
$S_{NOp,2}$	gN/m^3	8.54	8.35	4.27	4.00	0.28	0.23
$S_{Op,2}$	$gCOD/m^3$	3.93	3.98	2.97	2.99	1.10	0.96
$S_{NH,2}$	gN/m^3	0.69	0.55	0.89	0.72	3.3	3.00

Appendix B

Table A2. Peterson matrix for the reduced ASM1 model with 9 state variables.

Component →	***i***	**1**	**2**	**3**	**4**	**5**	**6**	**7**	**8**	**9**	**Process Rate, ρ_j [M L^{-3} T^{-1}]**
j	**Process ↓**	S_S	X_S	$X_{B,H}$	$X_{B,A}$	S_O	S_{NO}	S_{NH}	S_{ND}	X_{ND}	
1	Aerobic growth of heterotrophs	$-\frac{1}{Y_H}$		1		$-\frac{1-Y_H}{Y_H}$		$-i_{XB}$			$\hat{\mu}_H\left(\frac{S_S}{K_S+S_S}\right)\left(\frac{S_O}{K_{O,H}+S_O}\right)X_{B,H}$
2	Anoxic growth of heterotrophs	$-\frac{1}{Y_H}$		1			$-\frac{1-Y_H}{2.86\,Y_H}$	$-i_{XB}$			$\hat{\mu}_H\left(\frac{S_S}{K_S+S_S}\right)\left(\frac{K_{O,H}}{K_{O,H}+S_O}\right)\left(\frac{S_{NO}}{K_{NO}+S_{NO}}\right)\eta_g X_{B,H}$
3	Aerobic growth of autotrophs				1	$-\frac{4.57-Y_H}{Y_H}$	$\frac{1}{Y_A}$	$-i_{XB}-\frac{1}{Y_H}$			$\hat{\mu}_A\left(\frac{S_{NH}}{K_{NH}+S_{NH}}\right)\left(\frac{S_O}{K_{O,A}+S_O}\right)X_{B,A}$
4	'Decay' of heterotrophs		$1-f_p$	-1						$i_{XB}-f_P i_{XP}$	$b_H X_{B,H}$
5	'Decay' of autotrophs		$1-f_p$		-1					$i_{XB}-f_P i_{XP}$	$b_A X_{B,A}$
6	Ammonification of soluble organic nitrogen							1	-1		$k_a S_{ND} b_H X_{B,H}$
7	'Hydrolysis' of entrapped organics	1	-1								$k_H\frac{X_S/X_{B,H}}{K_X+(X_S/X_{B,H})}\left[\left(\frac{S_O}{K_{O,H}+S_O}\right)+\eta_h\left(\frac{K_{O,H}}{K_{O,H}+S_O}\right)\left(\frac{S_{NO}}{K_{NO}+S_{NO}}\right)\right]X_{B,H}$
8	Hydrolysis' of entrapped organic nitrogen								1	-1	$\rho_7\left(\frac{X_{ND}}{X_S}\right)$
Observed conversion rates [M L^{-3} T^{-1}]		$r_i=\sum_j v_{ij}\rho_j$									
Stoichiometric Parameters: Heterotrophic yield: Y_H, Autotrophic yield: Y_A, Fraction of biomass yielding particulate products: f_P, Mass N/Mass COD in biomass: i_{XB}, Mass N/Mass COD in products from biomass: i_{XP}		Readily biodegradable substrate [M (COD) L^{-3}]	Slowly biodegradable substrate [M (COD) L^{-3}]	Activate heterotrophic biomass [M (COD) L^{-3}]	Activate autotrophic biomass [M (COD) L^{-3}]	Oxygen (negative COD) [M (COD) L^{-3}]	Nitrate and nitrite nitrogen [M (N) L^{-3}]	NH^+_4 + NH_3 nitrogen [M (N) L^{-3}]	Soluble biodegradable organic nitrogen [M (N) L^{-3}]	Particulate biodegradable organic nitrogen [M (N) L^{-3}]	Kinetic Parameters: Heterotrophic growth and decay: $\hat{\mu}_H$, K_S, $K_{O,H}$, K_{NO}, b_H Autotrophic growth and decay: $\hat{\mu}_A$, K_{NH}, $K_{O,A}$, b_A Correction factor for anoxic growth of heterotrophs: η_g Ammonification: k_a Hydrolysis: k_h, K_X Correction factor for anoxic hydrolysis: η_h

Appendix C

Appendix C.1 PI Controllers for the Plant

The controlled plant has two control loops to perform the following actions:

1. Regulate the level of $S_{NOp,2}$ by manipulating Q_{ap}.

For this control loop, $S_{NOp,2}$ is the PV. With the corresponding SP being denoted by $spS_{NOp,2}$, e is expressed as: $e = spS_{NOp,2} - S_{NOp,2}$. Hence, $\dot{e} = -\dot{S}_{NOp,2}$. Substituting these terms in Equation (2), the controller equation for this control loop becomes:

$$\dot{Q}_{ap} = K_{c,p1}\left(-\dot{S}_{NOp,2} + \frac{1}{\tau_{Ip1}}\left(spS_{NOp,2} - S_{NOp,2}\right)\right) \tag{A5}$$

where $\dot{S}_{NOp,2}$ is taken from the ODE corresponding to the mass balance of $S_{NOp,2}$ in the second anoxic reactor of the plant.

2. Regulate the level of $S_{Op,5}$ by manipulating $(K_L a)_p$.

For this control loop, $S_{Op,5}$ is the PV. With the corresponding SP being denoted by $spS_{Op,5}$, e is expressed as: $e = spS_{Op,5} - S_{Op,5}$. Hence, $\dot{e} = -\dot{S}_{Op,5}$. Substituting these terms in Equation (2), the controller equation for this control loop becomes:

$$\left(\dot{K}_L a\right)_p = K_{c,p2}\left(-\dot{S}_{Op,5} + \frac{1}{\tau_{Ip2}}\left(spS_{Op,5} - S_{Op,5}\right)\right) \tag{A6}$$

where, $\dot{S}_{Op,5}$ is taken from the ODE corresponding to the mass balance of $S_{Op,5}$ in the third aerobic reactor of the plant.

Appendix C.2 PI Controller Equations for the Model

The controlled model has the control loops to perform the following actions:

1. Regulate the level of $S_{NO,1}$ by manipulating Q_a

For this control loop, $S_{NO,1}$ is the PV. With the corresponding SP being denoted by $spS_{NO,1}$, e is expressed as: $e = spS_{NO,1} - S_{NO,1}$. Hence, $\dot{e} = -\dot{S}_{NO,1}$. Substituting these terms in Equation (2), the controller equation for this control loop becomes:

$$\dot{Q}_a = K_{c,1}\left(-\dot{S}_{NO,1} + \frac{1}{\tau_{I1}}\left(spS_{NO,1} - S_{NO,1}\right)\right) \tag{A7}$$

where, $\dot{S}_{NO,1}$ is taken from the ODE corresponding to the mass balance of $S_{NO,1}$ in the first reactor of the model.

2. Regulate the level of $S_{O,2}$ by manipulating $K_L a$

For this control loop, $S_{O,2}$ is the PV. With the corresponding SP being denoted by $spS_{O,2}$, e is expressed as: $e = spS_{O,2} - S_{O,2}$. Hence, $\dot{e} = -\dot{S}_{O,2}$. Substituting these terms in Equation (2), the controller equation for this control loop becomes:

$$\dot{K}_L a = K_{c,2}\left(-\dot{S}_{O,2} + \frac{1}{\tau_{I1}}\left(spS_{O,2} - S_{O,2}\right)\right) \tag{A8}$$

where, $\dot{S}_{O,2}$ is taken from the ODE corresponding to the mass balance of $S_{O,2}$ in the second reactor of the model.

References

1. Kumar, M.D.; Tortajada, C. *Assessing Wastewater Management in India*, 1st ed.; Springer: Singapore, 2020; pp. 53–58.
2. Ozgun, H.; Cicekalan, B.; Akdag, Y.; Koyuncu, I.; Ozturk, I. Comparative evaluation of cost for preliminary and tertiary municipal wastewater treatment plants in Istanbul. *Sci. Total Environ.* **2021**, *778*, 146258. [CrossRef] [PubMed]
3. Keerio, H.A.; Bae, W. Experimental Investigation of Substrate Shock and Environmental Ammonium Concentration on the Stability of Ammonia-Oxidizing Bacteria (AOB). *Water* **2020**, *12*, 223. [CrossRef]
4. Capodaglio, A.G.; Olsson, G. Energy issues in sustainable urban wastewater management: Use, demand reduction and recovery in the urban water cycle. *Sustainability* **2020**, *12*, 266. [CrossRef]
5. Drewnowski, J.; Remiszewska-Skwarek, A.; Duda, S.; Łagód, G. Aeration process in bioreactors as the main energy consumer in a wastewater treatment plant. Review of solutions and methods of process optimization. *Processes* **2019**, *7*, 311. [CrossRef]
6. Drewnowski, J. Advanced supervisory control system implemented at full-scale WWTP—A case study of optimization and energy balance improvement. *Water* **2019**, *11*, 1218. [CrossRef]
7. Borzooei, S.; Campo, G.; Cerutti, A.; Meucci, L.; Panepinto, D.; Ravina, M.; Riggio, V.; Ruffino, B.; Scibilia, G.; Zanetti, M. Optimization of the wastewater treatment plant: From energy saving to environmental impact mitigation. *Sci. Total Environ.* **2019**, *691*, 1182–1189. [CrossRef]
8. Muoio, R.; Palli, L.; Ducci, I.; Coppini, E.; Bettazzi, E.; Daddi, D.; Fibbi, D.; Gori, R. Optimization of a large industrial wastewater treatment plant using a modeling approach: A case study. *J. Environ. Manag.* **2019**, *249*, 109436. [CrossRef]
9. Elawwad, A.; Matta, M.; Abo-Zaid, M.; Abdel-Halim, H. Plant-wide modeling and optimization of a large-scale WWTP using BioWin's ASDM model. *J. Water Process Eng.* **2019**, *31*, 100819. [CrossRef]
10. Vergara-Araya, M.; Hilgenfeldt, V.; Peng, D.; Steinmetz, H.; Wiese, J. Modelling to lower energy consumption in a large WWTP in China while optimising nitrogen removal. *Energies* **2021**, *14*, 5826. [CrossRef]
11. Caraman, S.; Luca, L.; Vasiliev, I.; Barbu, M. Optimal-setpoint-based control strategy of a wastewater treatment process. *Processes* **2020**, *8*, 1203. [CrossRef]
12. El bahja, H.; Vega, P.; Revollar, S.; Francisco, M. One layer nonlinear economic closed-loop generalized predictive control for a wastewater treatment plant. *Appl. Sci.* **2018**, *8*, 657. [CrossRef]
13. Sadeghassadi, M.; Macnab, C.J.B.; Gopaluni, B.; Westwick, D. Application of neural networks for optimal-setpoint design and MPC control in biological wastewater treatment. *Comput. Chem. Eng.* **2018**, *115*, 150–160. [CrossRef]
14. Boruah, N.; Roy, B.K. Event triggered nonlinear model predictive control for a wastewater treatment plant. *J. Water Process Eng.* **2019**, *32*, 100887. [CrossRef]
15. Zhang, A.; Liu, J. Economic MPC of wastewater treatment plants based on model reduction. *Processes* **2019**, *7*, 682. [CrossRef]
16. Revollar, S.; Vega, P.; Vilanova, R.; Francisco, M. Optimal control of wastewater treatment plants using economic-oriented model predictive dynamic strategies. *Appl. Sci.* **2017**, *7*, 813. [CrossRef]
17. Zhang, Y.; Monder, D.; Fraser Forbes, J. Real-time optimization under parametric uncertainty: A probability constrained approach. *J. Process Control* **2002**, *12*, 373–389. [CrossRef]
18. Chachuat, B.; Srinivasan, B.; Bonvin, D. Adaptation strategies for real-time optimization. *Comput. Chem. Eng.* **2009**, *33*, 1557–1567. [CrossRef]
19. Chen, C.Y.; Joseph, B. On-line optimization using a two-phase approach: An application study. *Ind. Eng. Chem. Res.* **1987**, *26*, 1924–1930. [CrossRef]
20. Ahmad, A.; Singhal, M.; Gao, W.; Bonvin, D.; Engell, S. Enforcing Model Adequacy in Real-Time Optimization via Dedicated Parameter Adaptation. *IFAC-Pap.* **2018**, *51*, 49–54. [CrossRef]
21. Roberts, P.D. Coping with model-reality differences in industrial process optimisation—A review of integrated system optimisation and parameter estimation (ISOPE). *Comput. Ind.* **1995**, *26*, 281–290. [CrossRef]
22. Marchetti, A.; Chachuat, B.; Bonvin, D. Modifier-adaptation methodology for real-time optimization. *Ind. Eng. Chem. Res.* **2009**, *48*, 6022–6033. [CrossRef]
23. Chachuat, B.; Marchetti, A.; Bonvin, D. Process optimization via constraints adaptation. *J. Process Control* **2008**, *18*, 244–257. [CrossRef]
24. Alex, J.; Benedetti, L.; Copp, J.; Gernaey, K.; Jeppsson, U.; Nopens, I.; Pons, M.-N.; Steyer, J.-P.; Vanrolleghem, P. *Benchmark Simulation Model No. 1 (BSM1)*; University of Lund: Lund, Sweden, 2008.
25. Karia, G.L.; Christian, R.A. *Wastewater Treatment: Concepts and Design Approach*; Prentice-Hall of India Pvt. Ltd.: New Delhi, India, 2013; pp. 1–11.
26. Tejaswini, E.S.S.; Panjwani, S.; Seshagiri Rao, A. Design of Hierarchical Control Strategies for Biological Wastewater Treatment Plants to Reduce Operational Costs. *Chem. Eng. Res. Des.* **2020**, *161*, 197–205. [CrossRef]
27. Zhang, A.; Yin, X.; Liu, S.; Zeng, J.; Liu, J. Distributed Economic Model Predictive Control of Wastewater Treatment Plants. *Chem. Eng. Res. Des.* **2019**, *141*, 144–155. [CrossRef]
28. Qiao, J.; Zhang, W. Dynamic Multi-Objective Optimization Control for Wastewater Treatment Process. *Neural Comput. Appl.* **2016**, *29*, 1261–1271. [CrossRef]
29. Han, H.-G.; Zhang, L.; Liu, H.-X.; Qiao, J.-F. Multiobjective Design of Fuzzy Neural Network Controller for Wastewater Treatment Process. *Appl. Soft Comput.* **2018**, *67*, 467–478. [CrossRef]

30. Morales-Rodelo, K.; Francisco, M.; Alvarez, H.; Vega, P.; Revollar, S. Collaborative Control Applied to BSM1 for Wastewater Treatment Plants. *Processes* **2020**, *8*, 1465. [CrossRef]
31. Henze, M.; Grady, C.P.L., Jr.; Gujer, W.; Marais, G.V.R.; Matsuo, T. *Activated Sludge Model no 1*; IAWPRC: London, UK, 1987.
32. Takács, I.; Patry, G.G.; Nolasco, D. A dynamic model of the clarification-thickening process. *Water Res.* **1991**, *25*, 1263–1271. [CrossRef]
33. Waller, K.V.; Makila, P.M. Chemical reaction invariants and variants and their use in reactor modeling, simulation, and control. *Ind. Eng. Chem. Process Des. Dev.* **1981**, *20*, 1–11. [CrossRef]
34. Seborg, D.E.; Edgar, T.F.; Mellichamp, D.A.; Doyle, F.J., III. *Process Dynamics and Control*, 3rd ed.; John Wiley & Sons, Inc.: Hoboken, NJ, USA, 2011; ISBN 9780470128671.
35. Biegler, L.T. *Nonlinear Programming: Concepts, Algorithms, and Applications to Chemical Processes*; Society for Industrial and Applied Mathematics: Philadelphia, PA, USA, 2010; pp. 181–212.
36. Krishnamoorthy, D.; Foss, B.; Skogestad, S. Steady-state real-time optimization using transient measurements. *Comput. Chem. Eng.* **2018**, *115*, 34–45. [CrossRef]
37. De Avila Ferreira, T.; Wuillemin, Z.; Marchetti, A.G.; Salzmann, C.; Van Herle, J.; Bonvin, D. Real-time optimization of an experimental solid-oxide fuel-cell system. *J. Power Sources* **2019**, *429*, 168–179. [CrossRef]
38. De Avila Ferreira, T.; François, G.; Marchetti, A.G.; Bonvin, D. Use of transient measurements for static real-time optimization. *IFAC-Pap.* **2017**, *50*, 5737–5742. [CrossRef]
39. Zamouche, R.; Bencheikh-Lehocine, M.; Meniai, A.-H. Oxygen transfer and energy savings in a pilot-scale batch reactor for domestic wastewater treatment. *Desalination* **2007**, *206*, 414–423. [CrossRef]
40. Marchetti, A.; François, G.; Faulwasser, T.; Bonvin, D. Modifier adaptation for real-time optimization—Methods and applications. *Processes* **2016**, *4*, 55. [CrossRef]
41. Andersson, J.A.E.; Gillis, J.; Horn, G.; Rawlings, J.B.; Diehl, M. CasADi: A Software Framework for Nonlinear Optimization and Optimal Control. *Math. Program. Comput.* **2018**, *11*, 1–36. [CrossRef]
42. Arismendy, L.; Cárdenas, C.; Gómez, D.; Maturana, A.; Mejía, R.; Quintero, M.C.G. Intelligent System for the Predictive Analysis of an Industrial Wastewater Treatment Process. *Sustainability* **2020**, *12*, 6348. [CrossRef]
43. Wang, D.; Thunéll, S.; Lindberg, U.; Jiang, L.; Trygg, J.; Tysklind, M.; Souihi, N. A Machine Learning Framework to Improve Effluent Quality Control in Wastewater Treatment Plants. *Sci. Total Environ.* **2021**, *784*, 147138. [CrossRef]
44. Xie, Y.; Chen, Y.; Lian, Q.; Yin, H.; Peng, J.; Sheng, M.; Wang, Y. Enhancing Real-Time Prediction of Effluent Water Quality of Wastewater Treatment Plant Based on Improved Feedforward Neural Network Coupled with Optimization Algorithm. *Water* **2022**, *14*, 1053. [CrossRef]